

REPORT DOCUMENTATION PAGE

*Form Approved
OMB No. 0704-0188*

Public reporting burden for this collection of information is estimated to average 1 hour per response, including the time for reviewing instructions, searching existing data sources, gathering and maintaining the data needed, and completing and reviewing this collection of information. Send comments regarding this burden estimate or any other aspect of this collection of information, including suggestions for reducing this burden to Department of Defense, Washington Headquarters Services, Directorate for Information Operations and Reports (0704-0188), 1215 Jefferson Davis Highway, Suite 1204, Arlington, VA 22202-4302. Respondents should be aware that notwithstanding any other provision of law, no person shall be subject to any penalty for failing to comply with a collection of information if it does not display a currently valid OMB control number. **PLEASE DO NOT RETURN YOUR FORM TO THE ABOVE ADDRESS.**

1. REPORT DATE (DD-MM-YYYY)		2. REPORT TYPE		3. DATES COVERED (From - To)	
4. TITLE AND SUBTITLE				5a. CONTRACT NUMBER	
				5b. GRANT NUMBER	
				5c. PROGRAM ELEMENT NUMBER	
6. AUTHOR(S)				5d. PROJECT NUMBER	
				5e. TASK NUMBER	
				5f. WORK UNIT NUMBER	
7. PERFORMING ORGANIZATION NAME(S) AND ADDRESS(ES)				8. PERFORMING ORGANIZATION REPORT NUMBER	
9. SPONSORING / MONITORING AGENCY NAME(S) AND ADDRESS(ES)				10. SPONSOR/MONITOR'S ACRONYM(S)	
				11. SPONSOR/MONITOR'S REPORT NUMBER(S)	
12. DISTRIBUTION / AVAILABILITY STATEMENT					
13. SUPPLEMENTARY NOTES					
14. ABSTRACT					
15. SUBJECT TERMS					
16. SECURITY CLASSIFICATION OF:		17. LIMITATION OF ABSTRACT	18. NUMBER OF PAGES	19a. NAME OF RESPONSIBLE PERSON	
a. REPORT	b. ABSTRACT			c. THIS PAGE	19b. TELEPHONE NUMBER (include area code)

Final Report

for

BRG-053; Boron Nanotubes/Nanofibers in Propellant Material Formulations: Testing and Characterization for Gun Barrel Protection

**And Modification No. 1 to Ordnance Technology Initiative No. 1; BRG-
053
Ordnance Technology Base Agreement No. 2009-618**

Reporting Period: September 20, '09 – December, '10

Ordnance technology Initiative Team

Initiative Lead: Zafar Iqbal

Other Initiative Team Member:
Jinwen Liu

Initiative Team Technical POC

Name: Zafar Iqbal
Company: CarboMet, LLC
Street Address: 18 Erskine Drive
City, State, Zip Code: Morristown, New Jersey 07960
Phone Number: 973 476 3404
Email address: iqbazafar@gmail.com

Submitted: 01/13/2011

Boron nanotube/nanofiber synthesis - Abstract

A novel, facile and cost-effective approach to the synthesis of boron nanostructures comprising of a mixture of boron nanotubes (BNTs) and nanofibers (BNFs) was developed under this contract. A method of nitrogen doping the BNTs and BNFs was also demonstrated. A key feature of this work is the use of a solid instead of a gaseous boron precursor for the synthesis of boron nanotubes and boron nanofibers. A solid boron precursor was chosen for BNT/BNF synthesis because typical gaseous boron precursors (e.g. BCl_3 and B_2H_6) used in prior work are either corrosive or energetic compounds. This would require special handling for safety reasons which would complicate the synthesis process, particularly in scaled up operations. Two solid boron precursors, MgB_2 and $\text{Mg}(\text{BH}_4)_2$, were used in the synthesis performed as discussed in detail below. Because of the e-beam instability of the boron nanostructures prepared using $\text{Mg}(\text{BH}_4)_2$, further work needs to be done in characterizing samples made by this method and completing the downselection of the process to be used for scaled up synthesis to provide prototype samples to the US Army ARDEC for testing in propellant formulations.

Synthesis using MgB_2 as boron precursor:

The small scale synthesis of boron nanotubes/nanofibers was carried out using the following method: MgB_2 (Alfa Aesar Company) powder as boron precursor, Ni_2B (99%, GFS Chemicals) powder as the primary catalyst, and mesostructured hexagonal framework MCM-41(Sigma Aldrich) zeolite powder as the template for guiding growth of tubes and fibers, with a mass ratio of 5:3:2 was placed in a quartz boat after being ground using a mortar and pestle to micrometer-range particle sizes. This mass ratio of precursor (MgB_2), catalyst (Ni_2B) and template/support (MCM-41) was found to produce the highest concentration of boron nanotubes/boron nanofibers (BNTs/BNFs) based on scanning electron microscope analysis (SEM) after carrying out a series of experiments with different ratios. The optimal reaction temperature of 950°C was determined by carrying out the reaction at different temperatures ranging from 800° to 1000°C followed by scanning electron microscope analysis. The mixed powder was placed in a quartz boat that was introduced into an 80-cm long, 2.5-cm diameter quartz reactor tube inside a computer-controlled electric furnace which is part of a chemical vapor deposition system connected to an oil bubbler at the exit end. The tube was pumped down to 1×10^{-3} Pa and then back-filled with pure argon at a flow rate of 150 standard cubic centimeters per minute (sccm). The furnace was heated to 950°C at the rate of $10^\circ\text{C}/\text{min}$ and kept at this temperature for 60 minutes. The system was then cooled down to room temperature under argon flow. A dark powder was obtained which was removed from the boat and purified by suspending in 2M sodium hydroxide solution, sonicated for 30 minutes to wash away the MCM-41 template and then vacuum filtered to obtain the pure product.

SEM images of as-prepared samples from MgB_2 at 950°C before and after purification are shown in Figure 2. Extensive growth of the nanostructures out of the MCM-41 zeolite is evident in the left image. The image on the right shows that nearly all the MCM-41 is removed from the sample.

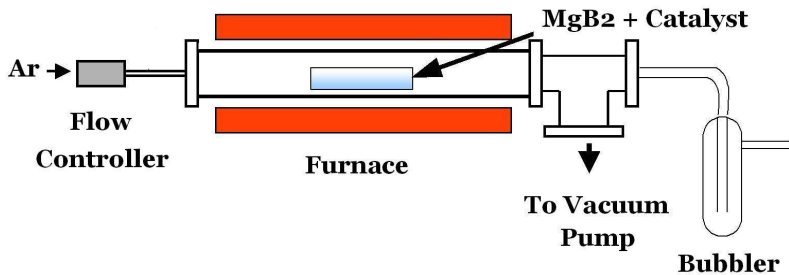


Figure 1. Small scale chemical vapor deposition setup used for the synthesis of BNTs and BNFs.

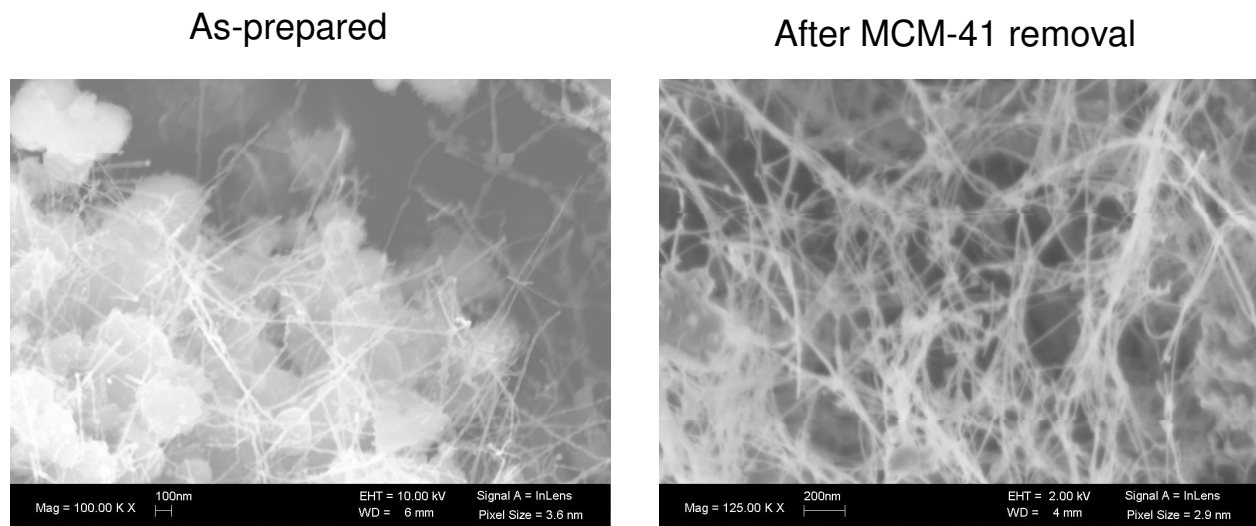


Figure 2. (Left panel) SEM image of BNTs mixed with BNFs prepared from MgB₂ at 950°C before purification using 2M NaOH; and (Right) SEM image of the sample in the left panel after purification.

Extensive characterization of the samples prepared from MgB₂ using the method described above were carried out at different resolutions by FE-SEM (field emission-scanning electron microscopy) and TEM (transmission electron microscopy) together with EELS (electron energy loss spectroscopy) and EDS (energy dispersive x-ray spectroscopy) microanalyses. BNTs were differentiated from BNFs by high resolution TEM as discussed below. Figures 3(a) and 3(b) show FE-SEM images at two spatial resolutions from partially purified samples. The relatively straight BNTs, which are abundant in quantity and range in diameter between about 10-30 nm and up to a few micrometers in length, appear to grow out from the MCM-41 template. However, the diameters observed are much larger than those of the approximately 4 nm pores in MCM-41 suggesting that the growth involves a more complex mechanism than simple templating. The structures produced are stable in the electron beam both in SEM and TEM (see below) in contrast to instability under electron beam irradiation observed in ca. 4 nm diameter single wall BNTs prepared by Ciuparu et al [1]. Bulbous tips indicated by arrows in Figure 2(b) are typical features of the nanotubular structures. Similar features were observed in boron nitride nanotubes synthesized by Lourie et al [2].

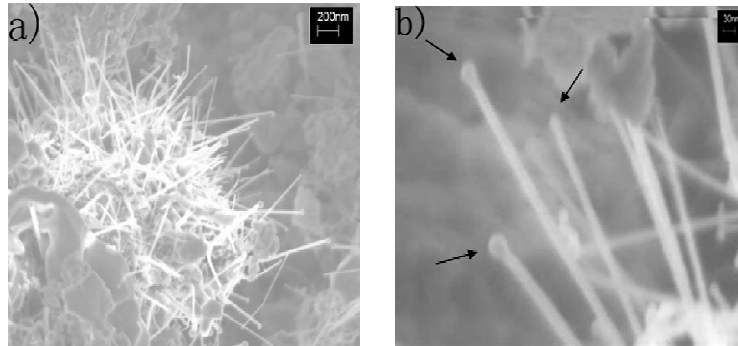


Figure 3. (a) FE-SEM image of BNTs and BNPs appearing to grow out from the MCM-41 template in large quantities from a partially purified sample. The tubes are mostly straight and appear to be stable in the electron beam; and (b) Higher resolution FE-SEM image showing bulbous tips (arrowed) formed on the tubular structures.

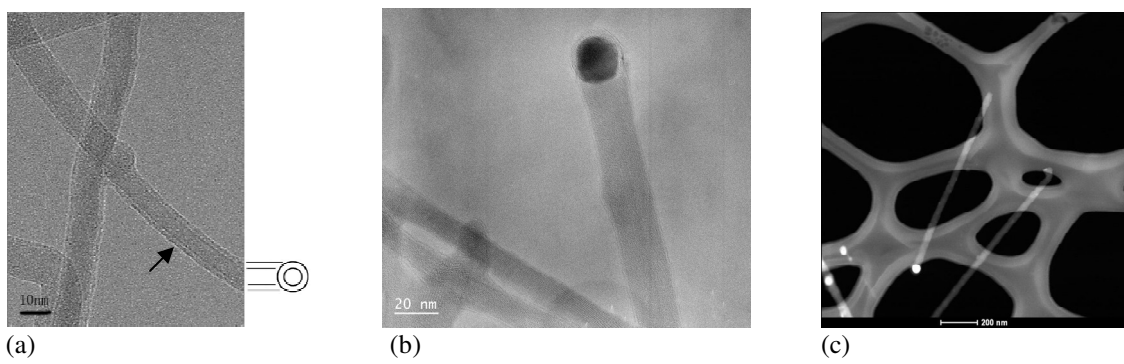


Figure 4. (a) TEM image of a double-walled BNT (arrowed) with a diameter of 10 nm – also shown schematically in insert to the right; (b) TEM image showing a tilted 20 nm diameter BNT on the right, and two 10 nm BNPs lying flat on the TEM substrate on the bottom left of the image; and (c) Dark field TEM image of very straight BNTs that are bent upwards at the tips and showing contrast at the tips due to the presence of metallic catalyst particles (also see EDS data in Figure 6).

TEM images of highly purified samples are shown in Figure 4. Figure 3(a) shows a double-walled BNT structure with a diameter of 10 nm. Figure 3(b) depicts a vertical BNT which is 20 nm in diameter. On the lower left of this image lying flat on the grid are two 10 nm BNPs. Lattice fringes are observed on the sidewalls of the nanostructures. This suggests that the nanotubes and nanofibers produced are crystalline consistent also with the observation of selected area electron diffraction patterns from the samples. Figure 3(c) shows a dark field image of very straight BNTs lying on the holey carbon grid with their tips curved upwards. Sharp image contrast evident at the tips is due to the presence of metallic catalyst particles, consistent with the EDS data discussed below. EELS (Electron Energy Loss Spectroscopy) data (Figure 5) taken from a nanotube sidewall show the boron K-edge spectrum with three primary features – a pre-peak shoulder at 190 eV, a peak at 193 eV and a broad signal near 200 eV associated with boron bonded to oxygen. Neither the Ni_L edge (around 850 eV) nor the Mg_K edge (around 1300 eV) is observed consistent with the EDS data discussed below.

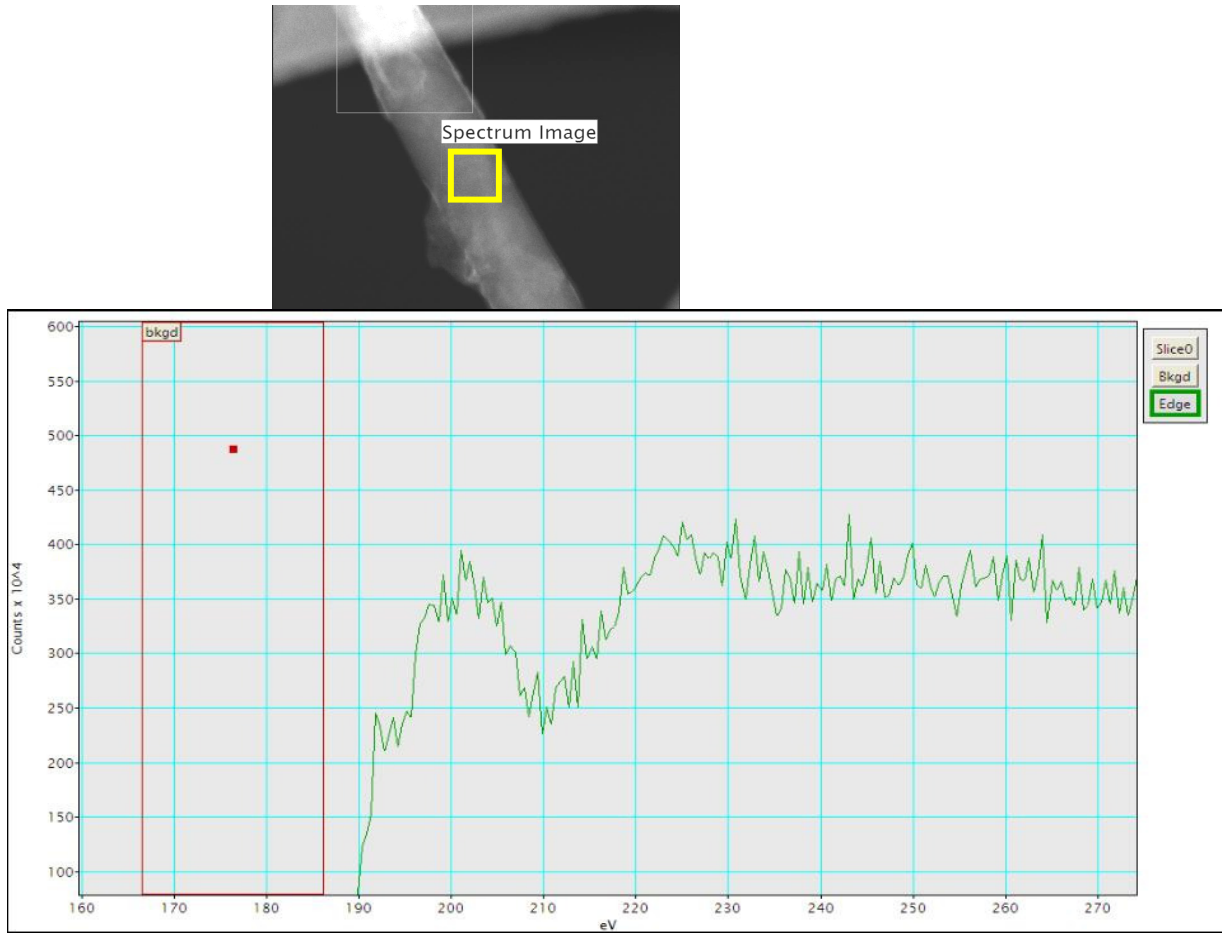
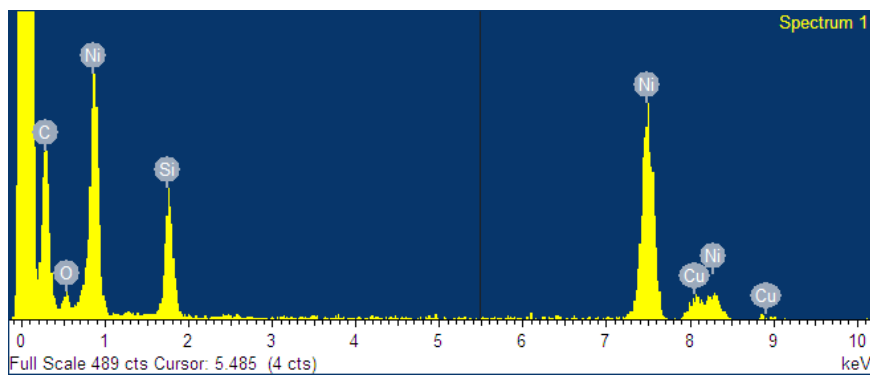


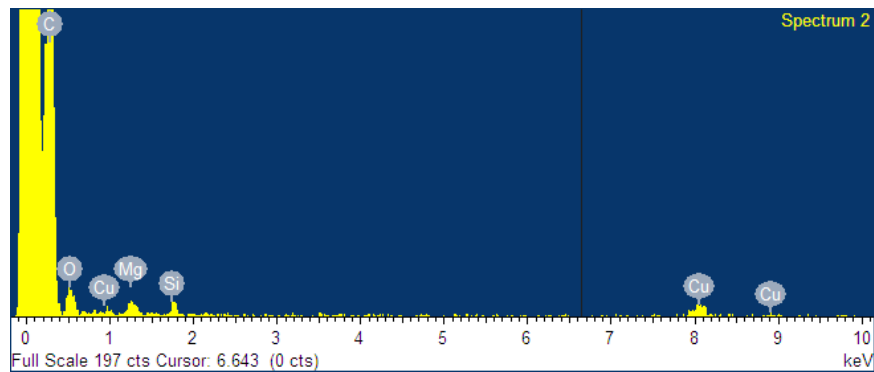
Figure 5. (Top) TEM image of BNT sidewall showing the area indicated in yellow from which the EELS data were collected; and (Bottom) Electron energy loss spectrum showing counts $\times 10^4$ versus energy in eV from the area indicated in the top panel.

presence of Ni from the Ni_2B catalyst. No magnesium is found at the tips, but surprising Si, probably due to partial decomposition of the MCM-41 template, is detected. EDS taken on the sidewall away from the tip shows only traces of Mg catalyst and Si, and Ni is not observed. Before use in propellant formulations the BNTs will therefore have to undergo a second purification step with dilute acid to remove the nickel at the tips. Raman spectra have been obtained on purified samples using 633 nm excitation and are similar to the spectrum reported by Xu et al [3] for boron nanoribbons as shown in Figure 7.

The BNTs obtained in this work are larger in diameter and longer than the single wall boron nanotubes reported by Ciuparu et al [1]. Moreover, the fact that the diameters of the BNTs and BNFs synthesized are larger than the approximately 4 nm diameter of the pores in MCM-41 and the BNT tips contain nickel suggests that growth is initiated within the pores and progresses to outside the pores via a vapor-liquid-solid (VLS) process as observed for boron nanowires by Wang et al [4].



(a)



(b)

Figure 6. EDS taken in the TEM from the tip (a) and from the sidewall (b) of the BNT shown in Figure 4(c).

Synthesis using Mg(BH₄)₂ as boron precursor:

Scale up to gram quantities in a batch process was conducted using Mg(BH₄)₂ as the boron precursor combined with efficient ball milling in acetone or alcohol. The mechanical ball-milling time was found to be most efficient at 6 hrs whereas the mass ratio was optimal at 6:3:2 for precursor, catalyst and support, respectively. The best temperature for the process was found to be 750° - 850°C. The rest of the process was conducted as described above for the small scale synthesis using MgB₂. FE-SEM images from as-prepared half-gram quantities indicated extensive growth of BNTs/BNFs in a fibrous and web-like morphology. The web-like morphology is particularly evident for the sample in the FE-SEM image shown in Figure 8 grown at 750°C.

By contrast to BNTs/BNFs produced from Mg(BH₄)₂, those produced from MgB₂ grow at 950°C and are straighter and shorter as discussed above. This is likely to be due to the fact that nascent hydrogen is produced in the reaction zone when Mg(BH₄)₂ is used as the boron precursor similar to the synthesis reported by the Yale group [1] where gaseous BCl₃ mixed with hydrogen gas is used as the precursor. Hydrogen produced in this reaction passivates the unsaturated boron atoms and stabilizes the electron-deficient boron structures formed, thus allowing for larger quantities of BNTs/BNFs to be produced rapidly.

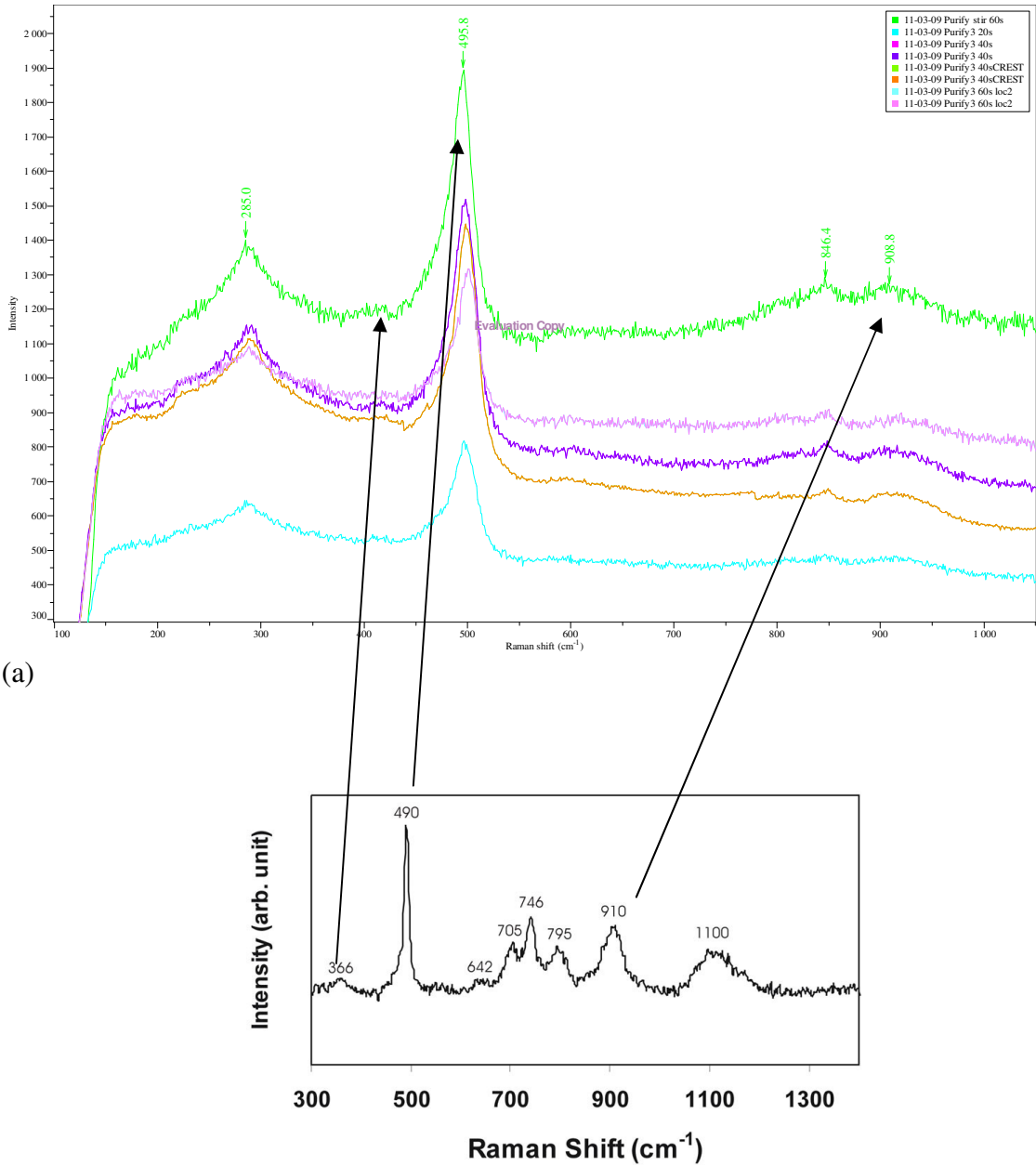


Figure 7. (a) Raman spectra of different regions of a BNT/BNF sample compared with the Raman spectrum obtained for a sample boron nanoribbons by Xu et al [3] (b). Arrows point to Raman lines in boron nanoribbons also seen in BNTs and BNFs, particularly the strong line at about 490 cm^{-1} .

The BNTs/BNFs produced from $\text{Mg}(\text{BH}_4)_2$ approach diameters below 10 nm or 3.6 nm reported by the Yale group [1]. This is consistent with the instability observed in the electron beam by these BNTs and BNFs similar to that reported by the Yale group [1]. Getting transmission electron microscope (TEM) images of these samples may therefore be challenging but maybe achieved at relatively low resolution using low voltage TEM or scanning TEM (STEM).

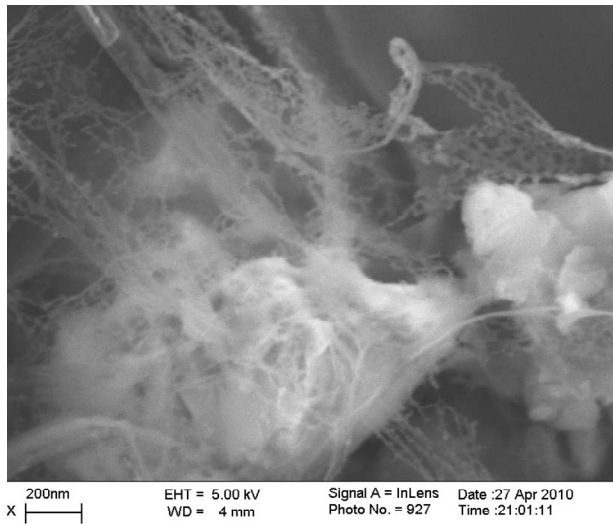


Figure 8. FE-image from a 0.5 gm sample made from $\text{Mg}(\text{BH}_4)_2$ at 750°C in flowing argon with Ni_2B as catalyst and MCM-41 as template showing extensive web and fiber-like growth of boron nanotubes/nanofibers.

Nitrogen-doped BNTs/BNFs

Nitrogen doped BNTs and BNFs are likely to provide robust boron nitride coatings during propellant firing to protect gun barrel surfaces. Also since the nitrogen doped nanostructures remain highly electrically and thermally conducting unlike pure boron

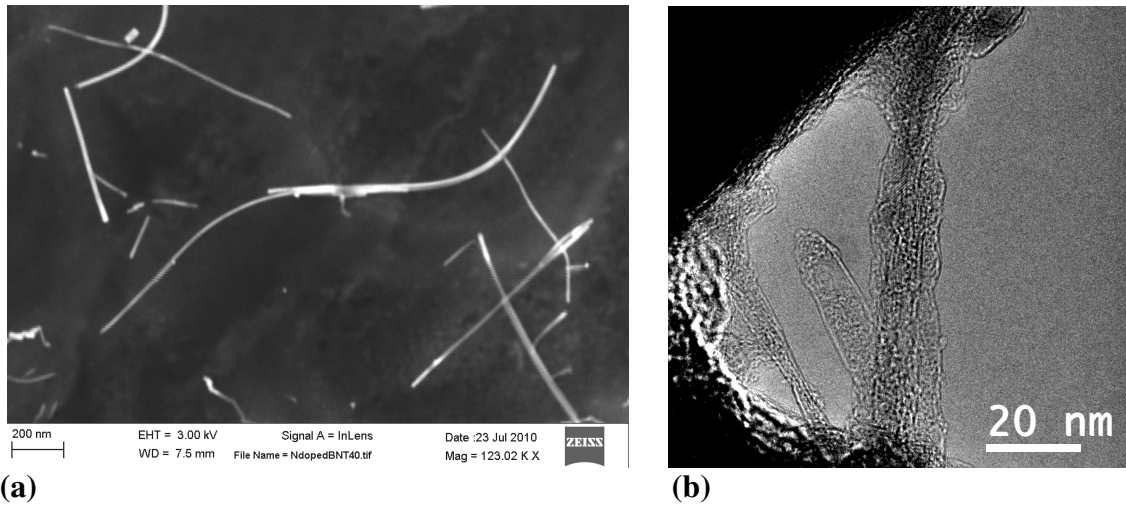
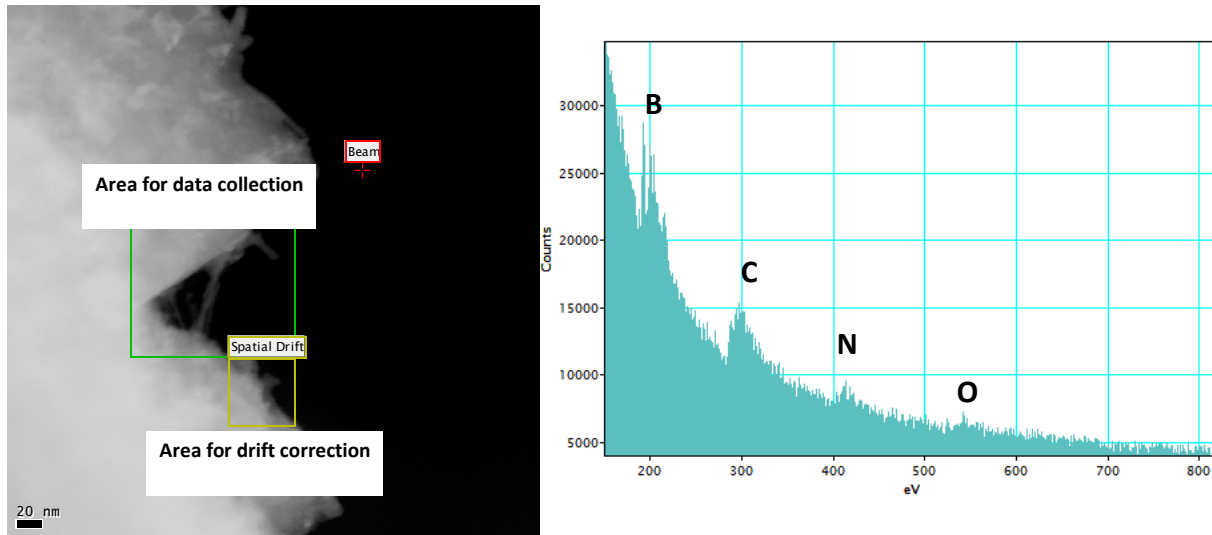


Figure 9. (a) SEM image of BNTs on a TEM grid from a sample prepared at 950°C from MgB_2 in argon mixed with 5% ammonia; and (b) TEM from BNTs in the same grid.



(a)

(b)

Figure 10. (a) TEM image from a region in the same grid shown in Figure 9; and (b) EELS from the area shown indicating electron energy loss from B and N. Features due to carbon and oxygen are from the holey carbon grid and oxygen on the boron nanotube sidewalls.

nitride nanotubes, which is insulating, they would provide protection against the formation of hot spots and charging-induced accidental initiation in propellant formulations. Nitrogen doped boron nanotubes would therefore be highly attractive additives for the formulation of insensitive munitions.

A number of strategies for nitrogen doping BNTs and BNFs were used. The best so far has been the use of ammonia mixed with argon during synthesis to provide nascent nitrogen for doping the BNT/BNF sidewalls. When MgB_2 is used in the synthesis the temperature of $950^\circ C$ employed would be sufficient to decompose ammonia to produce nitrogen and hydrogen without use of a catalyst. However, when $Mg(BH_4)_2$ is used with synthesis temperatures in the $750^\circ - 850^\circ C$ range, an iron nanopowder catalyst will be needed. SEM and TEM images together with EELS data shown in Figures 9 and 10 support the formation of nitrogen doped BNTs. It is worth noting that the TEM image shows that the sidewalls of the nitrogen doped BNTs are more disordered than those for pure BNFs and BNFs depicted in Figure 4.

Scaled up synthesis:

BNT/BNF synthesis using $Mg(BH_4)_2$ appears more attractive than that using MgB_2 because of higher BNT/BNF yield, lower synthesis temperature and narrower diameter of the tubes and fibers. However, the current price of $Mg(BH_4)_2$ is higher than that of MgB_2 and more details about the structure of the nanotubes and nanofibers from $Mg(BH_4)_2$ has to be obtained.

If the $\text{Mg}(\text{BH}_4)_2$ method is downselected, large scale production of 10-100 gm quantities of BNTs/BNFs will be performed using a fluidized bed CVD vertical CVD temperature-controlled furnace system shown in Figure 11. The fluidization medium will consist of $\text{Mg}(\text{BH}_4)_2$ mixed by ball-milling with Ni_2B catalyst and MCM-41 template and the fluidization gas will be argon flowing approximately at 1000 sccm.

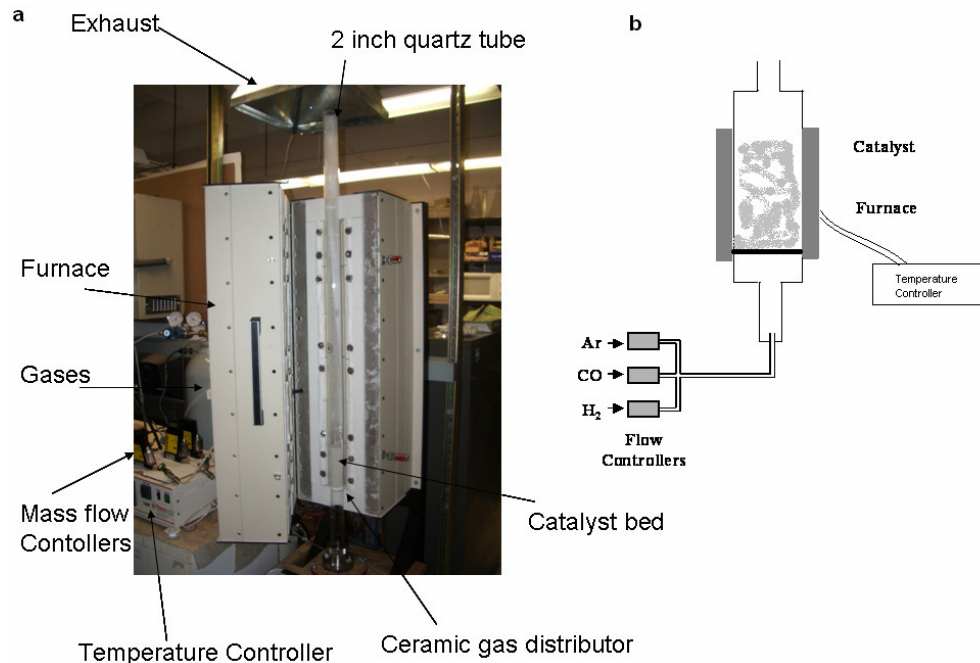


Figure 11. Scaled up vertical chemical vapor deposition furnace for pilot scale growth of BNTs/BNFs.

References:

1. D. Ciuparu, R. F. Klie, Y. Zhu and L. Pfefferle, *J. Phys. Chem. B* **108**, 3967 (2004).
2. O. R. Lourie, C. R. Jones, B. M. Bartlett, P. C. Gibbons, R. S. Ruoff and W. E. Buhro, *Chem. Mat.* **12**, 1808 (2000).
3. T.T. Xu, J-G. Zheng, N. Wu, A.W. Nicholls, J.R. Roth, D.A. Dikin and R.S. Ruoff, *Nano Lett.* **4**, 963 (2004).